AIAA JOURNAL
Vol. 38, No. 6, June 2000

Penetration and Spreading of Liquid Jets in an External–Internal Compression Inlet

T. Livingston* and C. Segal†
University of Florida, Gainesville, Florida 32611-6250
M. Schindler‡
University of Stuttgart, 70049 Stuttgart, Germany
and
V. A. Vinogradov§
Central Institute of Aviation Motors, 111250, Moscow, Russia

Injection of liquid fuel in the inlet of a vehicle flying at hypersonic speed is related to the development of liquid fuel-based supersonic-combustion ramjets as a means to increase the residence time and achieve partial fuel premixing prior to arrival at the combustion chamber. The strong liquid interaction with the inlet high-momentum airflow and shock wave system offers a mechanism for rapid jet and droplet breakup and, hence, improved mixing. The penetration and spreading of liquid jets in a two-dimensional external–internal compression inlet at Mach 3.5 using a noncombustible mixture that simulated the viscosity and surface tension of JP-10 was evaluated. Schlieren imaging has been used as the visualization technique for penetration studies, as well as light scattering for jet spreading. By using thin pylons to create a low-pressure region at the liquid injection station, the penetration increased compared with a nonpylon configuration while reducing the pressure losses associated with transverse jet injection. The pylons contributed to lift the liquid from the injection surface with less lateral spreading than the nonpylon-injection case, thus avoiding the presence of a low-speed combustible mixture in the inlet/isolator boundary layers and providing a mechanism to eliminate potential flashback.

Nomenclature

A = area (injection orifice, inlet capture, freestream), mm^2
d = injection orifice diameter, mm
H = inlet throat height, mm
L = inlet ramp length, mm
$\dot{m}$ = massflow, kg/s
Oh = Ohnesorge number, $\mu_l/(\rho_l \sigma d)^{0.5}$
q = dynamic pressure ratio
r = liquid/air density ratio
u = liquid/air velocity ratio
v = velocity, m/s
We = Weber number, $\rho_g v^2 d/\sigma$
δ = mixing layer growth
μ = dynamic viscosity, cP
ρ = density, kg/cm^3
ϕ = fuel/air equivalence ratio

Subscripts

c = inlet capture
g = gas
l = liquid
th = throat
0 = freestream value

Introduction

THE problem of achieving a high degree of fuel–air mixing in supersonic flows in residence-time-limited supersonic combustion ramjets, of the order of milliseconds, has received considerable attention with several mixing enhancing mechanisms studied to date. These include fuel injection configurations and generation of jet-air fluid mechanics interactions that enhance mixing. For high-speed applications some kind of parallel injection has been preferred over transverse injection due to lower pressure losses associated with jet injection. Among the proposed mixing configurations, straight or swept ramps have shown reasonable far-field mixing[1–3] despite lower near-field mixing when compared with transverse injection alternatives. The ramp vortex shedding provides a mechanism to lift the fuel from a low injection angle and promote penetration into the core air stream. A notable approach is the aerodynamic ramp[4,5] that consists of an array of wall injectors with various injection angles in both axial and lateral directions, simulating the physical ramp vortex generation by a number of fuel sources. The aerodynamic ramp eliminates the cooling requirements of physical ramps, especially in localized hot spots such as in recirculation regions. In the same time, the aerodynamic ramp is expected to reduce the drag while maintaining similar far-field mixing characteristics.

Other fluid interactions have been suggested to enhance mixing, among them vorticity generation by other means than ramps, for example, induced swirl and jet–shock wave interactions. Early studies of jets injected in subsonic and supersonic flows with vorticity generated by the presence of upstream aerodynamic profiles[6,7] indicated enhanced penetration and spreading due to the presence of vortical structures and induced jet swirl, resulting in improved mixing. Another mechanism that has shown improved gaseous jet mixing was the generation of vorticity by shock–jet interactions. A misalignment of pressure and density gradients caused by the presence of the shocks and nonsimilar jet-air densities results in a baroclinic torque[8,9] that induces vorticity and improved mixing. Owens et al.[10] found that the net effect of jet-shock interactions in a reacting, supersonic environment of liquid kerosene in air at Mach 1.8 was an increase in combustion efficiency as a result of enhanced mixing.

Although most of the studies mentioned involved gaseous fuels, in particular hydrogen, the issues of penetration and spreading for improved mixing apply as well when liquid fuels are used instead. Clear technological, economical, and operational advantages exist when liquid hydrocarbon fuels, such as kerosene, are used in comparison with hydrogen-based systems for the development of small

Received 10 March 1999; revision received 11 October 1999; accepted for publication 25 October 1999.

*Research Assistant, Department of Aerospace Engineering, Mechanics, and Engineering Science.

†Associate Professor, Department of Aerospace Engineering, Mechanics, and Engineering Science. Member AIAA.

‡Research Assistant, Luft- und Raumfahrttechnik.

§Head, Engine Gas Dynamic Department. Member AIAA.

hypersonic vehicles to Mach 8 (Ref. 11). However, the multistage physical–chemical processes of liquid hydrocarbon fuel burning, added to the short residence time available, increase the requirements for fast mixing. If the selected fuel is amenable to operate at supercritical conditions, a significant decrease in the time required for the liquid fuel breakup and vaporization can be achieved. Furthermore, if chemical decomposition accompanies these transformations, potential formation of hydrogen or other active radicals will result in an increased reactivity of the mixture and a reduction of the combustion length.

A simple evaluation of vaporized kerosene ignition time t_i showed that under typical conditions in a supersonic ramjet combustor (i.e., pressure $p = 50$–100 kPa and temperature $T = 600$–1000 K) $t_i = 5$–10 ms, and, therefore, the traditional methods of simple fuel injection for the hydrocarbon-based flames in supersonic flows are not effective. The experimental data of Goltsev et al.[12] indicated that the flame stability criterion for methane has been one order of magnitude lower than the corresponding value for hydrogen. In the case of the liquid fuel injection, the jet and droplet breakup along with vaporization are additional processes compared with the gaseous-based systems. The addition of active components such as hydrogen or ClF_3, SiH_4 compounds, etc.[13–15] to the fuel, as promoters, can reduce the induction time. This method is effective for the initiation of the combustion process but not for its stabilization during the flight because the proportion of added components may be up to 25%, thus increasing the volume and the complexity of the vehicle.[16] Additionally, some of these promoters may lead to a decrease in the specific impulse.

Another method of increasing the penetration, as a means of improving mixing, is the use of thin pylons that create a low-pressure region in their base. Transverse injection in this base would reduce the pressure losses associated with the jet injection by appropriate shaping of the pylons. Initial results of the effect of pylons on mixing and combustion have been presented by Vinogradrov and Prudnikov[17] and include a description of the plume geometry and penetration of a liquid kerosene jet behind a thin, swept pylon installed on the wall of the duct. The data indicated that it is possible to use this method for liquid injection along with the traditional methods employed to enhance mixing.[14,18]

To increase the fuel residence time and, thus, enhance the liquid fuel mixing, it is useful to inject part of the fuel in the isolator duct before the combustor or in the inlet and/or forebody of the vehicle. Successful application of fuel preinjection has been demonstrated in studies of external burning with the aim of providing control forces acting on the vehicle or decreasing the forebody or afterbody drag.[19]

Inlet fuel injection has shown the potential to decrease the mixing length by a factor of at least 1.5–2 for the typical ramjet with the design Mach number around 6 (Ref. 17). Furthermore, this method of injection may be accompanied by simultaneous thermal decomposition of the fuel and mixing enhancement through other means such as shock/spray interaction in the inlet flowfield.[20] The liquid injection configuration and flow rate have a strong effect on the supersonic inlet starting because the fuel injected upstream of the inlet capture modifies the flow past the inlet's external compression surface. The breakup of the fuel droplets, their mixing with the freestream flow, and evaporation may lead both to degradation and/or an improvement of the inlet starting and operational changes depending on the liquid fuel atomization process and the flight conditions. The inlet shock system, similar to the case of the gaseous fuel mixing,[10] may intensify the process of the droplet breakup (a secondary breakup mechanism) and fuel mixing upstream of the combustor intake.

Several practical issues arise in the case of preinjection of liquid fuel in the engine duct, including 1) mixing efficiency, flow deceleration, and inlet performance and 2) the ability to avoid flashback by eliminating the residence of the fuel on the inlet/isolator walls. If the pylons have the effect of lifting the fuel from the walls, thus avoiding the penetration of a combustible mixture in the boundary layers, the problem of flashback can be eliminated. In fact, previous combustion studies[21] have shown that injection of hydrogen behind pylons did not result in upstream interaction. Furthermore, along with the fuel injection scheme and the duct geometry, other parameters that affect the ignition delay time are important in preventing flashback, such as pressure, temperature, and mixture composition. For example, the fuel residence time at the static flow parameters within the inlet at $M_{\text{flight}} = 3.5$ is 0.4 ms, far shorter than the expected ignition delay time for JP-10 at this temperature and pressure. It is, thus, possible to achieve a certain degree of mixing without ignition within the inlet.

Note that certain beneficial effects could be obtained from the presence of fuel along the walls such as film cooling. It is estimated, however, that these beneficial effects are overcome by the potential danger of flashback and, in this case, the presence of fuel in the boundary layers along the walls of the inlet and isolator is undesirable.

This study shows the effects of the presence of pylons on the liquid fuel penetration and spreading in a two-dimensional, external–internal compression inlet in a Mach 3.5 airflow. Liquid jets with a diameter equal to the width of the pylons have been injected transverse to the flow in the base of the pylons. For all of the dynamic pressure ratios, the liquid penetrated immediately to the height of the pylons, then the jet column was abruptly broken and the liquid was carried into the inlet airflow. The pylons showed the capability to facilitate rapid liquid penetration into the airflow core, eliminating liquid arrival at the inlet's walls.

Experimental Setup

This study used the Mach 4 wind tunnel at the University of Florida, having a cross section of 15 × 15 cm and an optically accessible test-section length of 35 cm. Maximum steady-state regimes to 16 s are obtainable at Mach 3.5. Schlieren and light scattered images have been collected with a super-VHS camera, digitized in real time and synchronized with pressure measurements taken on the model via an electronic pressure scanner with 16 simultaneous recordings.

The inlet model is shown in Fig. 1. A 10-deg, $L = 22$-cm-long ramp includes a stagnation chamber from which liquid jets are injected at $0.28L$ from the leading edge. The inlet throat height H and the relative throat area A_{th}/A_c are 1.25 cm and 0.3, respectively. The total model length is 23 cm. At the exit a five-tube pressure rake

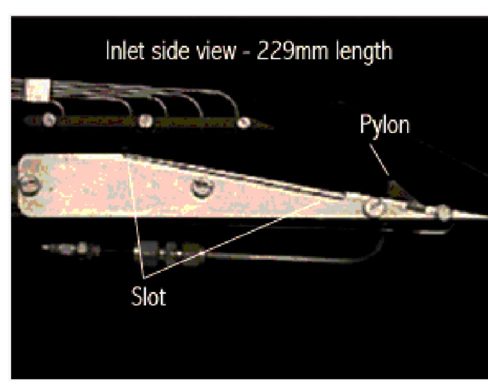

Fig. 1a Side view of the inlet: throat height 12.5 mm, ramp 10 deg; pylons have 30-deg and 10-mm height at the downstream location.

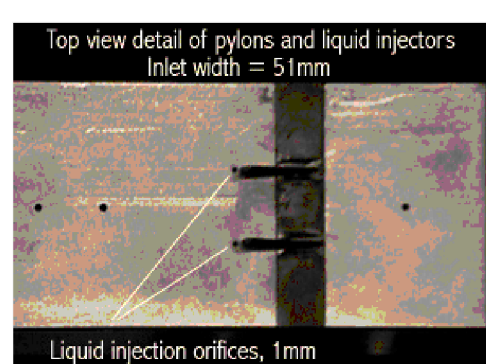

Fig. 1b Top view of injection orifices, 1 mm diameter, equally placed in a spanwise direction; pylons are 1 mm wide; first pressure ports on the ramp are also visible.

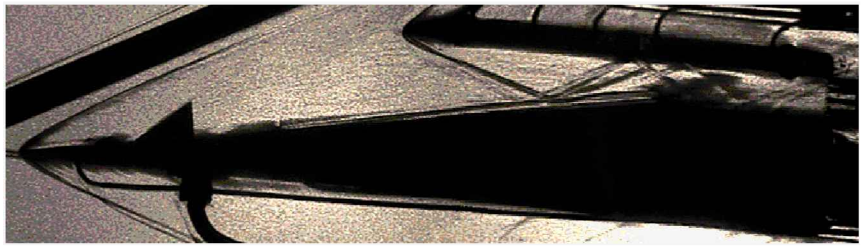

Fig. 2a Schlieren image of the inlet flowfield without liquid injection.

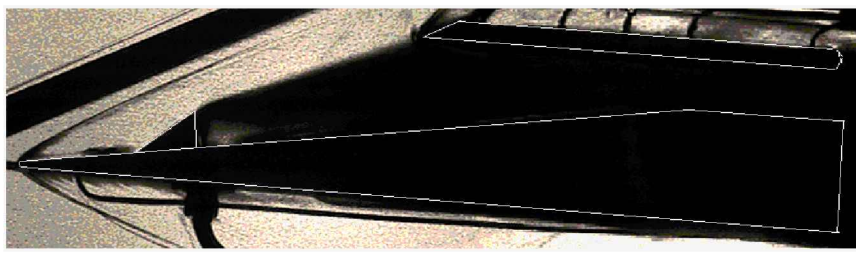

Fig. 2b Schlieren image with liquid injection at a m_l = 0.022 kg/s.

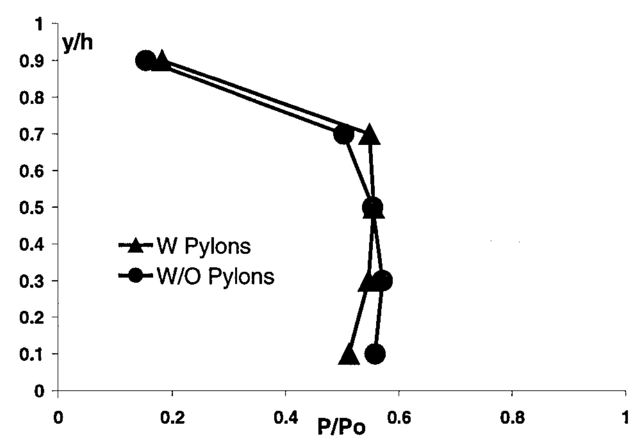

Fig. 2c Stagnation pressure at the inlet exit with and without pylons in the absence of liquid injection; presence of the pylons does not generate significant pressure losses in the inlet.

Table 1 Comparison of mixture properties

	Mixture	
Property	50% vol	JP-10
Density ρ, kg/cm^3	1.108	0.935–0.945
Viscosity μ, cP	4.57	4.0
Surface tension σ, mN/m	44.82	33.85

measures the inlet pressure recovery, a measure of pressure losses due to friction, mixing, and liquid–air interactions. Wall pressures are measured on the lower and upper walls of the model. A mixture of 50% volumetric commercial antifreeze in water has been used to delay the freezing of the liquid droplets beyond the inlet model. The resulting mixture has the properties listed in Table 1. For comparison, Table 1 includes the same parameters for JP-10, a high-energy-density fuel candidate for hypersonic applications. It can be seen in Table 1 that the mixture appears to be a reasonable substitute for the hydrocarbon for this type of experiment because it maintains similar parameters responsible for droplet breakup (i.e., Weber and Ohnesorge numbers) as JP-10. The liquid was injected transverse to the airflow from the base of low-drag pylons. The role of the pylons is to reduce the dynamic pressure of the air at the injection point, thus increasing the jet penetration. Each pylon had a 30-deg downstream wedge with a height of 10 and 1 mm constant thickness. The jet physical size was 1 mm (i.e., the pylon thickness) and was separated from the pylon by one jet diameter. The model sidewalls were made of plexiglass allowing optical access for the images presented hereafter. Longitudinal slots were cut in the inlet's side walls to allow air bleed and delay the onset of inlet unstart when large amounts of liquid were injected. The inlet was designed for a shock-on-lip operation without liquid injection at Mach 4. The experiments presented have been taken at Mach 3.5 sweeping the angle of attack (AOA) from +5 to −5 deg.

Results

Figures 2a and 2b show the flowfield throughout the entire inlet without and with liquid injection, respectively. The ramp leading edge shock is detached from the cowl lip due to operation at Mach 3.5, below the inlet design point of Mach 4. Therefore, $A_0/A_c < 1$. At a 5-deg AOA, theoretically, the shock will again anchor to the cowl lip, however, the finite thickness of the ramp's leading edge and the interactions with the oblique shocks generated by the side plates cause a deflection of the shock away from the inlet capture. The oblique shock formed at the cowl lip is reflected several times within the inlet. The line close to the ramp inside the inlet indicates the margins of the slots cut in the sidewalls to facilitate the inlet starting by allowing air bleed, necessary because the relative inlet throat, $A_{th}/A_c = 0.3$, is close to the theoretical required value of 0.31 for inlet starting at $M = 3.5$. These slots extend from downstream of the liquid injection to the inlet throat. As seen in Fig. 2, no significant effect on the inlet shock system is introduced by the presence of the pylons. The stagnation pressure measured at the inlet exit, shown in Fig. 2c, indicates as well that no significant pressure losses are induced by the presence of the pylons. However, they play an important role in reducing the dynamic pressure behind them resulting in increased liquid jet penetration. The double shock shown at the first reflection of the cowl lip shock indicates the internal shock reflection and the external shock transmitted through the bleed slot. Figure 2b shows the liquid penetration throughout the entire length of the inlet for a liquid-to-air mass flow ratio of 0.03. In this schlieren image, the liquid appears as a dark shade. The jets penetrate to the pylon's height at the injection location, then the liquid column is broken abruptly and the liquid is entrained by the airstream by counter-rotating vortices that develop in a streamwise direction.[22] Even at high liquid flow rate, as used in this case, corresponding to an equivalence ratio of $\phi = 0.45$, if JP-10 is the injected liquid, the liquid stream is entirely captured within the inlet entrance ensuring a practically complete cover of the vertical height of the inlet at the exit location. Despite these extreme operational conditions, the absence of liquid at the downstream base of the jets indicates the capability of the pylon configuration to lift the entire liquid off the surface. Farther downstream, due to increased pressure associated with inlet unstart, spreading is increased allowing the liquid to reach the sidewalls.

Evaluations of the boundary layer at the location of fuel injection indicated laminar conditions, thus, nonpylon injection caused separation. In the case of pylon injection, when the liquid jet was penetrated through the boundary-layer thickness (≈ 0.8–1 mm), that is, at small values of equivalence ratio $\phi < 0.3$ there was no boundary-layer separation. With $\phi > 0.35$ flow separation in the inlet can be observed, accompanied by a total pressure drop of 40–45% at the inlet exit. This situation is mostly due to the selection of a relative throat area close to the one required for inlet starting and the additional negative interaction of the initial shock wave with the boundary layer on the side walls. Thus, small amounts of fuel addition in the inlet caused large changes in the inlet flowfield. When separation appeared, some fuel penetrated through the three-dimensional separated zones to the side walls appearing in the two-dimensional image. It is expected that an increase of the relative inlet throat would provide nonseparated compression processes under large fuel flow rates injection behind the pylon.

Effect of Pylons

Figures 3a–3f show a comparison of jet penetration and spreading with and without the presence of pylons at selected AOA, that is, +5 and 0 deg. Figures 3a, 3b, 3e, and 3f represent schlieren images with the flow from left to right, and the fuel appears as dark regions. Figures 3c, 3d, 3g, and 3h show cross sections perpendicular to the flow using light scattering, thus, the liquid appears white on a black background.

Figure 3a shows clearly the removal of the jet entirely from the surface of the inlet ramp. In case of the nonpylon configuration, Fig. 3b, low penetration is initially noted, but it increases as the jet moves downstream into the inlet. Spreading images taken at the cowl station perpendicular to the ramp (see Figs. 3c and 3d), show a more concentrated liquid core for the pylon configuration than for the nonpylon case, with more spreading apparent in the nonpylon configuration. This is due to a more extensive separation of the boundary layer in comparison with the pylon configuration, and it does not constitute a desirable flow condition as the inlet operates at off-design conditions. In the presence of the pylon, most of the liquid is lifted off the surface without appreciable interaction with the boundary layer and is confined to the center of the duct. This is a guarantee against potential flashback caused by upstream propagation of the flame through the boundary layers. The effect of injection is appreciable in this case only because of the sensitivity of the inlet to throttling resulting from fuel addition and the interaction between the fuel plumes and the internal flow under conditions of a rather small relative inlet throat area. At the bottom of the liquid plume a three-dimensional effect of spillage through the inlet slots is evident by the entrainment of part of the fuel in a lateral direction in both pylon and nonpylon configurations (see Figs. 3c and 3d). No loss of mass is caused by this air bleed in the pylon configuration (Fig. 3c), however, the rapid spreading in the case of nonpylon configuration may cause some liquid mass loss through the inlet bleed (Fig. 3d). The situation is similar at AOA $=0$ deg as shown in Figs. 3e and 3f. Although no significant effect is noticeable in the schlieren penetration images (Fig. 3a vs Fig. 3e and Fig. 3b vs Fig. 3f, respectively) the spreading at AOA $=0$ (Figs. 3g and 3h) indicate that most of the liquid stays closer to the ramp, a result of a lower dynamic pressure ratio.

Figures 4a and 4b show the pressure distribution at the inlet exit for a +5- and 0-deg AOA. The injected liquid massflow and the corresponding dynamic pressure ratio q, defined as

$$q = \frac{\dot{m}^2 / A^2 \rho_l}{\gamma p_a M_a^2}$$

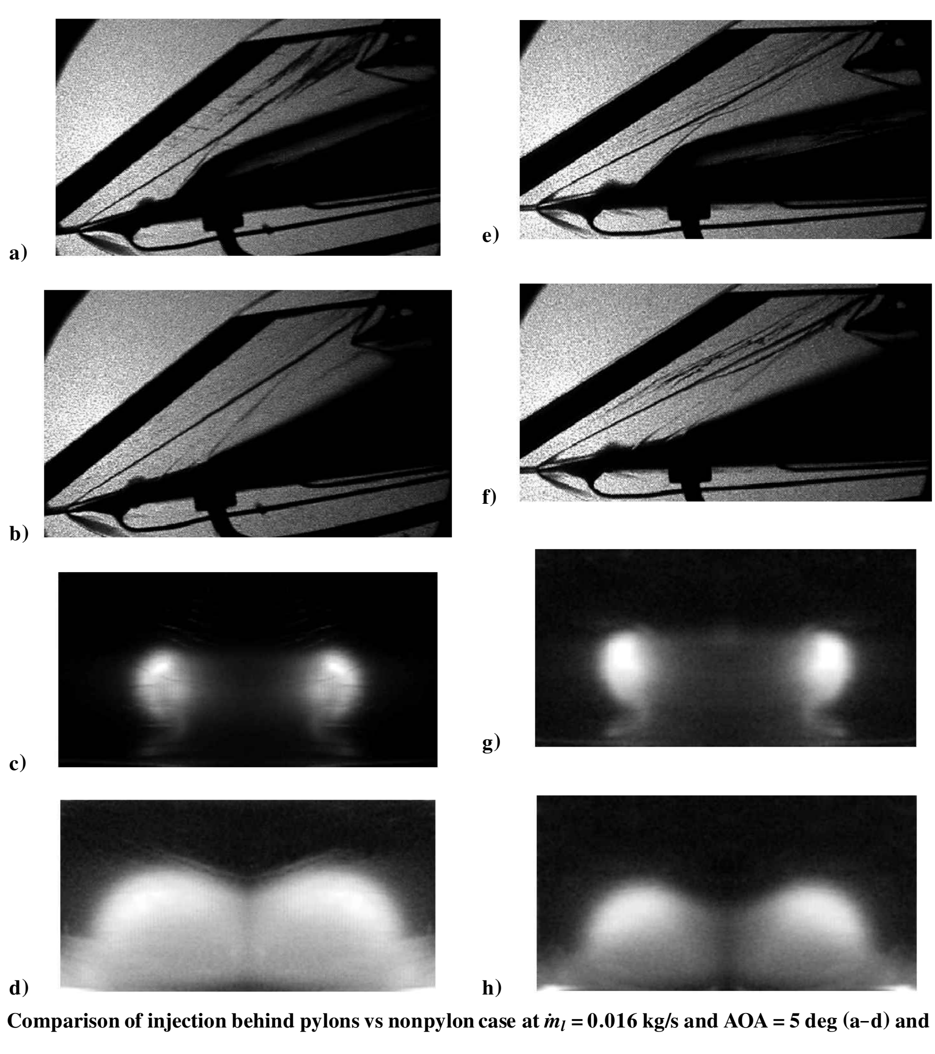

Fig. 3 Comparison of injection behind pylons vs nonpylon case at $\dot{m}_l = 0.016$ kg/s and AOA = 5 deg (a–d) and 0 deg (e–h).

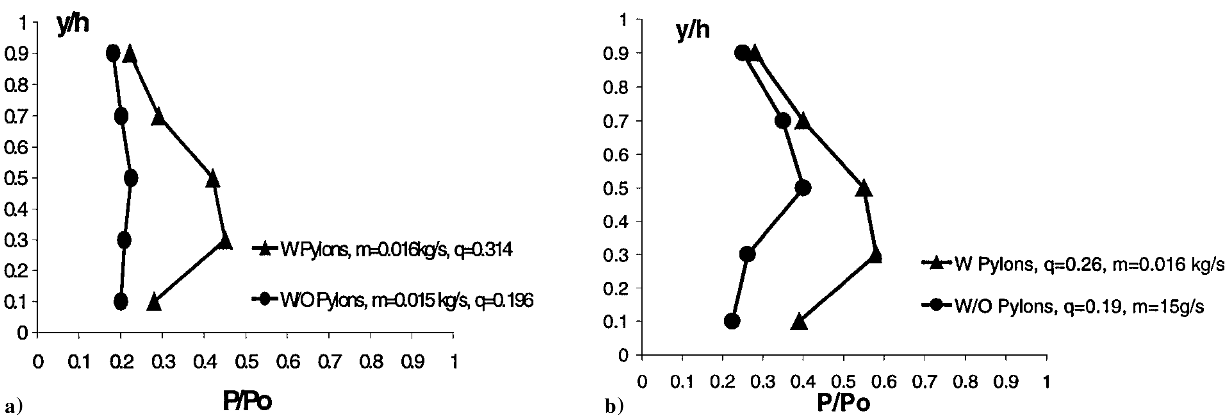

Fig. 4 Pressure distribution at the duct exit, at AOA = a) 5 and b) 0 deg.

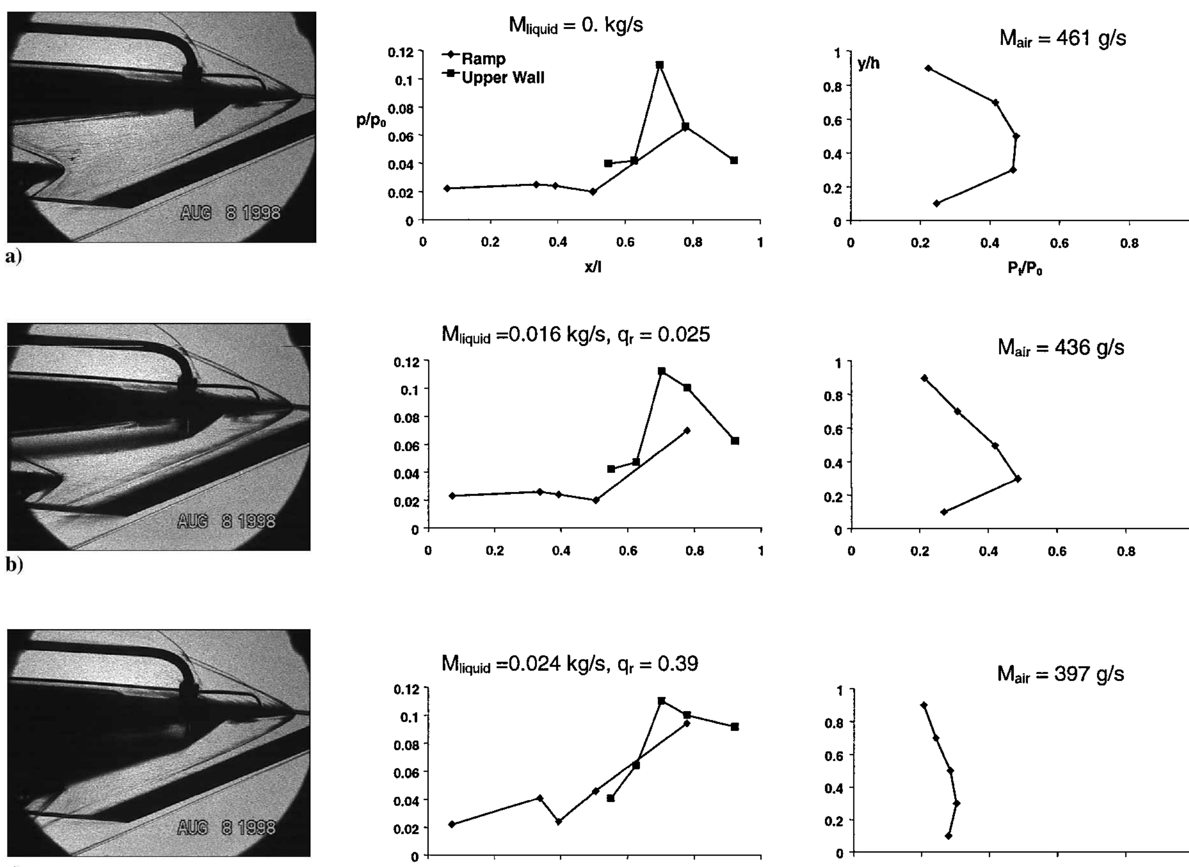

Fig. 5 Schlieren images (left), pressure distributions on the ramp and cowl (center) and rake pressures (right) for five selected liquid injection rates.

are indicated in Figs. 4a and 4b. Although the flow rate was $\dot{m}_l = 0.016$ kg/s in both cases, the presence of the pylons resulted in a higher dynamic pressure ratio due to reduced pressure in the pylon's base. The overall level of pressure at the inlet exit is higher with pylons at both positive angle of attack (see Fig. 4a) and AOA $= 0$. At AOA $= 0$ the upper inlet part indicates a drop in pressure recovery consistent with the presence of large amounts of liquid in the upper inlet region when the pylons are employed. The lower stagnation pressure recovery in the nonpylon configuration may be a result of more intensive impulse losses caused by flow separation in this configuration.

Effect of Massflow Rate on Pressure Recovery

Figures 5a–5c show the pressure distributions measured along the inlet ramp and on the cowl (center) and the stagnation pressure at the exit of the duct (right) for a range of liquid flow rates. Also shown are images collected at the same time instance with these pressure distributions (left). Three five-pitot probe rakes have been used to infer the momentum losses associated with liquid injection and calculate the air mass flow through the inlet. For airflow mass calculations three, five-probe rakes have been placed at the inlet exit. Air mass flows are indicated in the stagnation pressure profiles at the inlet exit (left column).

Figures 5b and 5c show the penetration of the liquid for several liquid flow rates, indicating increased penetration and jet spreading with increased q. The pressure plots, including the wall pressures as well as the stagnation rake at the inlet exit, indicate a drop in the airflow momentum associated with liquid injection, including shock–liquid interactions, mixing losses, and flow separation (in our case). This momentum loss can be compensated for in an engine equipped with this type of fuel injection scheme if the improved mixing would accelerate the physicochemical processes in the combustion chamber. These advantages have the potential to reduce the engine length, thus saving weight and reducing the friction losses and heat transfer loads. Furthermore, the mixing process in the inlet is more efficient than the similar process delayed for the combustion chamber because supersonic shear layer development depends on the density and velocity ratio of the two layers[23] r and u, respectively, as indicated by the following equation:

$$\delta \sim \frac{(1-u)\left(1+\sqrt{r}\right)}{1+u\sqrt{r}}$$

Both u and r are larger for the inlet and, therefore, a faster growth of the shear layer is expected.

The stagnation pressure for the no-injection case in Fig. 5a indicates the higher pressure at center of the duct than on the sides. This effect is due to the presence of both boundary layers and shock waves within the supersonic inlet. When liquid is injected, the center of the duct experiences a reduction in the stagnation pressure due to the momentum transfer from the airflow to the liquid. This pressure loss is associated with mixing losses and a certain amount of air mass flow is diverted from the inlet via spillage at the inlet capture and through the side slots. Note that the position of the oblique shock formed by the ramp does not change significantly, indicating low spillage and the capability of the side slots to modulate the inlet flow, thereby maintaining the inlet started over the entire range of liquid mass injection. The flow remains generically supersonic at the inlet exit, but the shock system strength is reduced resulting in a more uniform pressure distribution at this station. The air mass flow is reduced, as shown in Figs. 5 as a result of liquid addition and stagnation pressure drop. Because the leading shock wave in the schlieren images does not indicate any difference between the three flow rates it is expected that the airflow be reduced via increased bleed through the side slots. The effect of increasing the liquid injection rate on the total pressure recovery $P_{t,\mathrm{inj}}/P_{t,\mathrm{inj}=0}$ shown in Fig. 5 indicates that increasing the liquid flow rate past the on-design conditions when the inlet was started (see Fig. 5b) caused unstarting and a significant drop of pressure recovery from $P_{t,\mathrm{inj}}/P_{t,\mathrm{inj}=0} \approx 0.85$ to 0.55. This is an indication of the necessity to increase the inlet throat to prevent the extreme duct throttling that leads to flow separation and the possibility of flashback onset.

Summary

Liquid has been injected in a supersonic inlet simulating fuel injection upstream of a supersonic combustion chamber behind thin pylons. The liquid injection behind pylons indicated the following effects on the inlet flowfield characteristics:

1) Injection of liquid in the low-pressure region in the base of the pylons resulted in liquid penetration straight to the pylon's height. Then the liquid plume was dispersed by the high momentum airflow and carried into the inlet. Despite their effectiveness in enhancing the jet penetration, the pylons had a negligible effect on the inlet flowfield.

2) The presence of the pylons reduced the pressure losses associated with liquid injection relative to the nonpylon configuration.

3) All of the liquid was lifted from the injecting surface with less spreading than in the nonpylon configuration. This was caused by a more intensive flow separation in the duct for moderate liquid mass flows. Large rates of liquid caused the inlet unstart. Once the unstart conditions occurred, at dynamic pressure ratios greater than 0.25, the liquid penetration continued to and occupied the entire inlet exit height.

4) There was a stagnation pressure loss of 15% at $\phi = 0.3$ accompanying the liquid injection due to the momentum exchange between the high-speed airflow and the liquid. This momentum exchange is expected to accelerate the droplet breakup and enhance mixing, potentially resulting in an increased efficiency of the entire system inlet-combustion chamber. When inlet unstart was observed, at $\phi = 0.45$, the stagnation pressure loss was close to 50%.

5) No significant effect on the liquid penetration was noticed when the inlet AOA was modified from 0 to 5 deg, but higher overall pressure losses were met at a 5-deg AOA due mostly to the stronger shocks generated by the cowl.

References

[1]Northam, G. B., Greenberg, I., Byington, C. S., and Capriotti, D. P., "Evaluation of Parallel Injector Configurations for Mach 2 Combustion," *Journal of Propulsion and Power*, Vol. 8, No. 2, 1992, pp. 491–499.

[2]Hartfield, R. J., Hollo, S. D., and McDaniel, J. C., "Experimental Investigation of a Swept Ramp Injector Using Laser-Induced Iodine Fluorescence," *Journal of Propulsion and Power*, Vol. 10, No. 1, 1994, pp. 129–135.

[3]Riggins, D. W., McClinton, C. R., Rogers, R. C., and Bittner, R. D., "Investigation of Scramjet Strategies for High Mach Number Flows," *Journal of Propulsion and Power*, Vol. 11, No. 3, 1995, pp. 409–418.

[4]Cox, S. K., Fuller, R. P., Schetz, J. A., and Walters, R. W., "Vortical Interaction Generated by an Injector Array to Enhance Mixing in Supersonic Flow," AIAA Paper 94-0708, Jan. 1994.

[5]Fuller, R. P., Wu, P.-K., Nejad, A. S., and Schetz, J. A., "Fuel-Vortex Interaction for Enhanced Mixing in Supersonic Flow," AIAA Paper 96-2661, July 1996.

[6]Swithenbank, J., and Chigier, N. A., "Vortex Mixing for Supersonic Combustion," *Twelfth Symposium (International) on Combustion*, Combustion Inst., Pittsburgh, PA, 1968, pp. 1153–1162.

[7]Povinelli, L. A., and Ehlers, R. C., "Swirling Base Injection for Supersonic Combustion Ramjets," *AIAA Journal*, Vol. 10, No. 9, 1972, pp. 1243, 1244.

[8]Marble, F. E., Hendricks, G. J., and Zukoski, E. E., "Progress Toward Shock Enhancement of Supersonic Combustion Processes," AIAA Paper 87-1880, June 1987.

[9]Marble, F. E., Zukoski, E. E., Jacobs, J. W., Hendricks, G. J., and Waitz, I. A., "Shock Enhancement and Control of Hypersonic Mixing and Combustion," AIAA Paper 90-1891, July 1990.

[10]Owens, M., Segal, C., and Auslender, A. H., "Effects of Mixing Schemes on Kerosene Combustion in a Supersonic Airstream," *Journal of Propulsion and Power*, Vol. 13, No. 4, 1997, pp. 525–531.

[11]Heiser, W. H., Pratt, D. T., Daley, D. H., and Mehta, U. B., *Hypersonic Airbreathing Propulsion*, edited by J. S. Przewieniecki, AIAA Education Series, AIAA, Washington, DC, 1994, pp. 507–512.

[12]Goltsev, V. F., Sverdlov, E. D., and Tulupov, Yu. N., "Combustion of Methane Flame in High Velocity Air Flow with Recirculation Zone," *Proceedings of the 3rd All-Union Workshop on Flame Structure*, Vol. 1, Siberian Branch of the Russian Academy of Science, Novosibirsk, Russia, 1991, pp. 147–151.

[13]Waltrup, P., "Liquid Fueled Supersonic Combustion Ramjets: A Research Perspective of the Past, Present, and Future," *Journal of Propulsion and Power*, Vol. 3, No. 6, 1987, pp. 515–524.

[14]Hunt, J. L., Johnston, P. J., and Cubbage, J. M., "Hypersonic Airbreathing Missile Concepts Under Study at Langley," AIAA Paper 82-0316, Jan. 1982.

[15]Diskin, C. S., and Northam, G. B., "Evaluation of a Storable Fluorine-Based Pilot for Scramjet," AIAA Paper 86-0372, Jan. 1986.

[16]Bonghi, L., Dunlap, M. J., Owens, M. G., Young, C., and Segal, C., "Hydrogen Piloted Energy for Supersonic Combustion of Liquid Fuels," AIAA Paper 95-0730, Jan. 1995.

[17]Vinogradov, V. A., and Prudnikov, A. G., "Injection of Liquid into the Strut Shadow at Supersonic Velocities," SAE Aerospace Atlantic Conf., Society of Automotive Engineers, SAE-931455, Dayton, OH, April 1993.

[18]Kay, I. W., Peschke, W. T., and Guile, R. N., "Hydrocarbon-Fueled Scramjet Combustor Investigation," AIAA Paper 90-2337, July 1990.

[19]Tretyakov, P. K., Fomin, V. M., and Yakovlev, V. I., "New Principles of Control of Aerophysical Processes. Research Development," *Proceedings (Part 2) of the International Conference on the Methods of Aerophysical Research*, Inst. of Theoretical and Applied Mechanics, Novosibirsk, Russia, 1986, pp. 210–220.

[20]Vasilev, V. I., Zakotenko, S. N., Krasheninnikov, S. J., and Stepanov, V. A., "Numerical Investigations of Mixing Augmentation Behind Oblique Shock Waves," *AIAA Journal*, Vol. 32, No. 2, 1994, pp. 311–316.

[21]Vinogradov, V. A., Grachev, V., Petrov, M., and Sheechman, J., "Experimental Investigation of Two-Dimensional Dual Mode Scramjet with Hydrogen Fuel at Mach 4...6," AIAA Paper 90-5269, 1990.

[22]Tillman, T. G., Patrick, W. P., and Patterson, R. W., "Enhanced Mixing of Supersonic Jets," *Journal of Propulsion and Power*, Vol. 7, No. 6, 1991, pp. 1006–1014.

[23]Papamoschou, D., and Roshko, A., "Observation of Supersonic Free Shear Layer," AIAA Paper 86-0162, Jan. 1986.

S. K. Aggarwal
Associate Editor